PROSPECTS FOR THE USE OF Ti^{3+}:AL_2O_3 LASERS IN ATMOSPHERIC STUDIES

G.A. Skripko

Refresher Course for Specialists of Different Branches of Industry,
Byelorussian Polytechnical Institute, Minsk
Received January 6, 1989

The optophysical and spectral-luminescent properties of Ti^{3+}:Al_2O_3 crystals as active rods for a basic laser source to be used in atmospheric studies have been investigated.

The most essential lasing properties of the material are considered and the feasibility of creating simple high-efficiency sources of tunable coherent radiation in the 0.3 to 5.0 μm spectral range capable of operating in various regimes is demonstrated. Prospects for developing Ti^{3+}:Al_2O_3 lasers using coherent, flash-lamp, solar, or electron-beam pumping are discussed.

INTRODUCTION

Atmospheric research appears to be one of the most promising application areas for advanced laser techniques,[1–5] whose development and wide use are directly related to progress in laser technology itself. The major laser characteristics critical for optical sounding systems are the following: output pulse power and energy, pulse repetition rate, laser spatial and temporal characteristics, and the capability of operating in different regimes. Also of great importance are such laser characteristics as the wavelength tuning range, linewidth and stability, and the possibility of obtaining polychromatic emission. Also essential are the following performance parameters: simplicity of operation, reliability, lifetime, size, weight, and cost. These numerous and, to a certain extent, conflicting requirements cannot be met by any one type of laser. Therefore, to solve different optical sounding problems, one has to use different lasers, each device exhibiting a particular set of output characteristics. The above considerations show that the problem of instrumentational support for atmospheric sensing is very complicated. A major step in the development of state-of-the-art equipment for atmospheric investigations would be the creation of a laser source that would, as far as possible, comply with the above requirements and would be, first of all, capable of operating in any spectral region of interest. Accordingly, of special interest within a large family of modern lasers are solid-state lasers with doped crystals, which are characterized by a number of favorable properties[6–9] which allow for their successful application to atmospheric studies.

In the context of the problem of constructing tunable solid-state lasers for atmospheric studies it would appear expedient to consider first the general trend found in the field under discussion. This trend reveals itself in the design and development of solid-state lasers of a new generation[10] characterized by a much higher efficiency and improved performance.

Advances in solid-state lasers have been achieved as a result of, the use of transition-metal ions instead of rare-earth ions to dope the crystals. The former have wide absorption and luminescence bands due to a peculiar interaction between the electronic states of the activating ions and the lattice modes. The wide absorption bands lead to a more efficient consumption of the pumping radiation from the flashlamps which significantly improves the efficiency of the corresponding laser systems. In the case of coherent excitation the absorption bandwidth makes the choice of the excitation source immaterial. The wide, homogeneously broadened luminescence bands impart a new quality to solid-state lasers, viz., tunability of the laser output radiation over a wide spectral range, which is extremely important for a large number of applications. This has been possible, so far, only with color-center lasers and different types of dye lasers.

Although the total number of active media has increased, only a few lasing materials which can be regarded as fundamental or basic are under intensive study. In other words, the tendency observed here is similar to that found in microelectronics which eventually put silicon in the forefront as the major material. It is still too early to say which material will play an active role in quantum electronics. However, we think that a serious candidate for this role is titanium-doped-sapphire. It is completely probable that after detailed and thorough investigations and engineering and design development this material may become basic for a large class of lasers satisfying a large number of practical needs.

This work is an attempt to examine the most important features of this new medium, Ti^{3+}:Al_2O_3, as a laser material, evaluate the characteristics of lasers developed based on it, discuss the most probable tendencies towards their improvement, and finally, substantiate the feasibility of constructing a primary

Ti^{3+}:Al_2O_3 laser which can provide the solution for a wide range of atmospheric sensing problems. The discussion presented below is based mainly on the results obtained at the Byelorussian Polytechnical Institute.

The first observations of lasing in titanium-doped sapphire by Moulton[11] and then by Soviet[12–14] and West-German[15] researchers initiated a series of investigations into the optophysical, spectral-luminescent, and lasing properties of the material. More than a hundred papers devoted to the study of the spectroscopic and lasing characteristics of Ti^{3+}:Al_2O_3 crystals have been published. The results obtained so far are discussed in detail in reviews 16 and 17. The present treatment will deal first of all with those properties of the material that could enable its use as a basic laser medium and also with those characteristics of the crystal that have hot been addressed or have been insufficiently tackled in the literature.

OPTOPHYSICAL AND SPECTRAL-LUMINESCENCE PROPERTIES OF Ti^3+:Al_2O_3 CRYSTALS

These include the general optophysical properties of Al_2O_3 and the spectral-luminescent characteristics of the titanium-doped sapphire crystals. The host crystal Al_2O_3 is not only the material that served as the basis for creating the first laser — the ruby (Cr^{3+}:Al_2O_3) laser — but it still remains one of the most useful materials in quantum electronics. This laser medium exhibits a unique combination of optophysical properties (see Table I) inherent in .practically all its doped varieties, in particular, in titanium sapphire.[16–17]

TABLE I.

Optophysical properties of the Al_2O_3 crystal

Density	3.99-4.01 g/cm^3
Hardness	1940-2200 kg/cm^2
Thermal conductivity at T=300 K	45 W/m· degree
at T=65 K	1040 W/m· degree
Melting point	2050°C
Refractive index	1.766-1.774
Birefringence	-0.008
Dispersion in the interval 687-431 nm	0.018
Threshold of optical breakdown for pulses of duration 20-50 ns	350-600 MW/cm^2

Thus, the Al_2O_3 crystal seems to be in one of the leading places among laser hosts for its thermal conductivity, hardness, and birefringence. It should be noted that titanium-sapphire also possesses high photo-, thermal, and radiative strength and long-term stability. Not the least of the factors which distinguish this material is the fact that the technology for growing this type of crystal has finally been brought to a, commercial level.[17] The spectroscopic properties of Ti^{3+}:Al_2O_3 crystals were studied long ago. However, investigations on the subject have become more intensive now that this medium has been shown to lase.[17,21,22]

Let us consider the energy structure of the titanium ion in the Al_2O_3 matrix and the spectroscopic characteristics of the material which determine its lasing properties. The fivefold degenerate ^2D ground state of Ti^{3+} ($3d^1$ electronic configuration) in the Al_2O_3 crystalline field is split into two states by its cubic component: the triply degenerate $^2T_{2g}$ lower state and a doubly degenerate ^2E_g upper state. Further removal of the degeneracy is related to the effect of the trigonal component of the crystalline field, the spin-orbit interaction, and the Jahn-Teller effect. The latter is of special importance since it has the greatest influence on the lasing potential of Ti^{3+}:Al_2O_3, primarily its tuning range. As a result, the upper level is split into two components (see Fig. 1), transitions from which are centered at λ_1 = 490 nm (ν_1 = 20410 cm^{-1}) and λ_2 = 550 nm (ν_2 = 18180 cm^{-1}) with halfwidths $\Delta\nu_1$ = 1300 cm^{-1} and $\Delta\nu_2$ = 1000^{-1} cm^{-1}, the value of splitting due to the Jahn-Teller effect is ΔE_{JT} = 2230 cm^{-1}, and the intensity ratio is 1(550)/1(490) = 1/3. Consequently, the absorption spectrum of Ti^{3+}: Al_2O_3 has the form of a broad band peaked at λ_{max} ~ 490 nm with a shoulder on the long-wavelength slope around 550 nm (see Fig. 2). This band spans most of the visible range from 400 to 600 nm, which allows one to use different lasers operating in this spectral region as pumping sources, for example, argon-ion lasers, copper-vapor lasers, the second harmonic of neodymium lasers, etc. Moreover, the broad absorption band of titanium sapphire also allows one to use radiation from incoherent optical sources such as the Sun and light-emitting or laser diodes for pumping. Since the $^2T_{2g} \rightarrow E_g$ transition is spin-allowed, the absorption cross-section in the center of the band is $6 \cdot 10^{-20}$ cm^2, which provides an absorption coefficient of up to 2 cm^{-1} at a dopant concentration ($3.3 \cdot 10^{19}$ cm^{-3}) of 0.1% by weight.

The luminescence spectrum of Ti^{3+}: Al_2O_3 (Fig. 2a) has the form of a broad, structureless, practically homogeneously broadened band. Its extremely large width which covers an interval about 3200 cm^{-1} is striking because it exceeds the corresponding values for $d \leftrightarrow d$ transitions in other ions, for instance, alexandrite, Cr^{3+}: $BeAl_2O_4$ (Ref. 23). This very useful advantage can be explained using the configurational diagram in Fig. 1.

Figure 1a shows the energy surfaces in configuration space for the upper ^2E_g and lower $^2T_{2g}$ states caused by the Jahn-Teller effect. For the upper state the energy surface has rotationa symmetry and has the shape of a Mexican hat while for the lower state the surface is formed by three intersecting vibronic paraboloids. Luminescence occurs due to transitions from the laser vibrational sublevel of the ^2E_g state (this minimum in configuration space has the form of a circle, as shown in Fig. 1a) to the vibrational sublevels of the lower electronic state $^2T_{2g}$. Depending on the position of the point on this circle from which the transition starts,

it terminates, due to its verticality (according to the Franck-Condon principle), at one or another vibrational sublevel of the lower electronic state with energies ranging from 200 to 4230 cm^{-1} (Fig. 1b). Thus, the luminescence spectrum is further broadened by 2230 cm^{-1}. As a consequence, the whole luminescence band out to the 1-of-maximum level extends from 600 to 1100 nm. We have measured the luminescence band wings and their behavior at different temperatures, and also the relaxation spectra (the wavelength dependence of the luminescence decay time $\tau_{lum} = f(\lambda)$). The measurements show that the long-wavelength tail of the luminescence band stretches out to 1.3–1.35 μm and its intensity and shape vary with temperature over wide ranges. No relaxation spectrum was observed, i.e., the luminescence lifetime remained constant in the 0.63 to 1.35 μm range (the measurements were carried out at room temperature; the measurement error was ≤ 10%). The cross-section of the lasing transition $^2E_g \rightarrow {}^2T_{2g}$ at the maximum of the gain band was $3.5 \cdot 10^{-19}$ cm^2 and $1.5 \cdot 10^{-19}$ cm^2 for the π- and τ-polarizations, respectively.

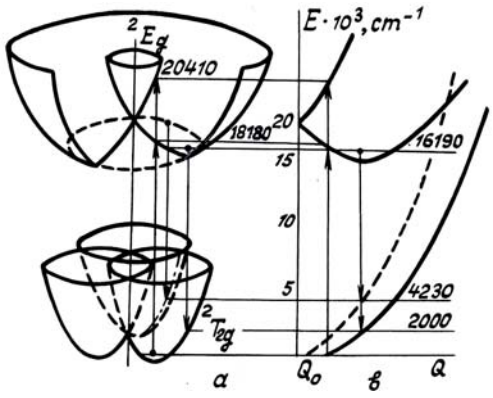

FIG. 1. Energy surfaces in configuration space due to the Jahn-Teller effect (a) and the plane configurational diagram for the Ti^{3+} ion in the Ti^{3+}: Al_2O_3 crystal (b). Energy is given in units of cm^{-1}.

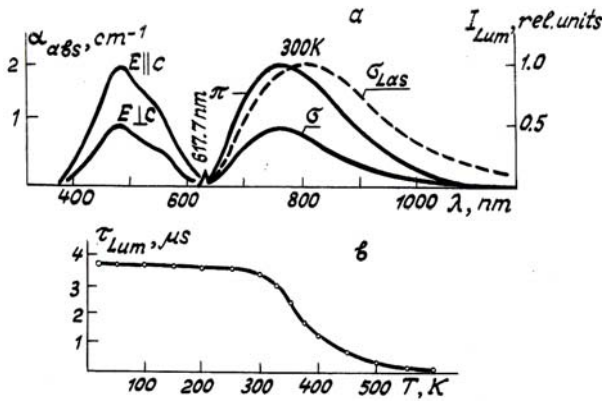

FIG. 2. Absorption and luminescence spectra and spectral behavior of the lasing transition cross-section (a); temperature dependence of the luminescence decay time for the Ti^{3+}:Al_2O_3 crystal (c = 0.1% by weight) (b).

The gain cross-section for one of the polarizations as a function of wavelength is described by the function[21]

$$\sigma(\mathbf{k}, \lambda) = \frac{\lambda^5 G(\mathbf{k}\lambda)}{hc^2 n^2}, \quad (1)$$

where $\sigma(\mathbf{k}, \lambda)$ is the gain cross-section at the wavelength λ in the direction of the vector $\vec{k}$; G is the spontaneous emission function which determines the radiation intensity per unit solid angle in the direction of the vector $\vec{k}$ per unit wavelength interval; h is Planck's constant; c is the velocity of light; and, n is the refractive index of the crystal.

Since luminescence relaxation does not depend on wavelength, it follows from Eq. (1) that the gain contour is shifted towards the long-wavelength region in comparison with the luminescence band, and its long-wave length wing is more developed (Fig. 2a). In fact, this means that, for a comparable luminescence intensity the gain in thelong-wavelength wing should dramatically exceed its value in the short-wave length region. Gain measurements in Ti^{3+}: Al_2O_3 for $\lambda > 1$ μm using second-harmonic radiation from a Nd^{3+}: YAG laser for excitation gave lasing transition cross-sections of $\sigma_{las} = 10^{-20}cm^2$ and $5 \cdot 10^{-21}$ cm^2 at $\lambda = 1.06$ and 1.15 μm, respectively. Note, for comparison, that the lasing transition cross-section for alexandrite at the peak of the gain band is $7 \cdot 10^{-21}$ cm^2 (Ref. 23). The above features enable one to predict the spectral range of the laser emission in titanium sapphire: first, it is much broader than would be expected on the basis of the luminescence spectrum.

It should be noted that the concrete spectral characteristics of crystals grown by different methods are noticeably different, being mostly determined by the growth and annealing techniques used.

Of the other spectroscopic properties inherent in Ti^{3+}: Al_2O_3 and characterizing it as a laser medium, we mention its high quantum yield of luminescence, the lack of absorption from the excited-state, and weak concentration quenching.

The quantum yield of luminescence at room temperature is > 80%. As the temperature is increased, nonradiative relaxation takes place and the quantum yield begins to fall along with the luminescence lifetime[28–29] (see Fig. 2b).

The lack of absorption from the excited state is characteristic of ions with the $3d^1(3d^9)$ configuration and conveniently distinguishes them from all other ions with vacant d-shells. This is because the first excited level of a $3d^1$-ion lies far above the ground level. Thus, for example, for Ti^{3+} it lies more than 80380 cm^{-1} above the ground state. Therefore, as a result of the splitting due to any real crystalline field, the resulting levels lie far from the upper laser level and can cause neither absorption from this level nor pumping radiation and, as a result, do not give rise to lasing. Thus, Ti^{3+}: Al_2O_3 is not burdened by one of the fundamental disadvantages that limits the lasing energy

and tuning range for all of the existing lasers based on chromium-doped crystals as well as lasers based- on crystals doped with V^{2+}, Co^{2+}, N^{2+}, Ce^{3+}, etc.

The effect of concentration quenching is not observed anywhere in the technologically attainable range of dopant concentrations.

LASING CHARACTERISTICS OF Ti^{3+}: Al_2O_3 LASERS

Let us consider first the lasing characteristics of coherently pumped Ti^{3+}: Al_2O_3 lasers which have provided the most promising results obtained so far. The usefulness of coherent excitation is occasioned by the availability of high-efficiency neodymium lasers integrated with nonlinear frequency converters for second-harmonic generation as well as the fairly well-studied argon and copper-vapor lasers.

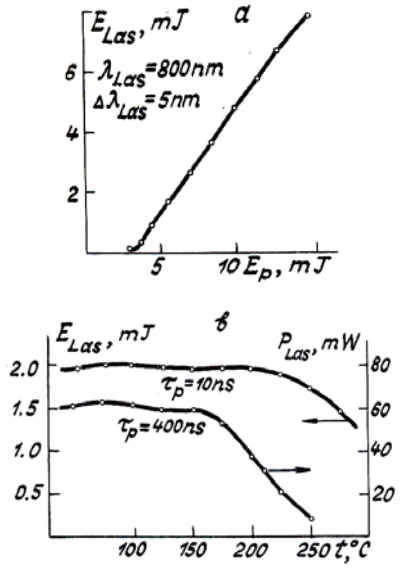

FIG. 3. Output energy as a function of pumping energy (a); temperature behavior of the energy and mean output power of Ti^{3+}: Al_2O_3 lasers pumped by the second harmonic of a Nd^{3+}: YAG laser (b).

A distinctive property of coherently pumped Ti^{3+}: Al_2O_3 lasers, demonstrated already in the early experiments,[13,22,24–30] is a high total conversion efficiency of up to 55–60%. Figure 3a presents an example of our data on the output energy of a repetitively pulsed Ti^{3+}: Al_2O_3 laser ($\bar{\lambda}$ = 800 nm) as a function of pumping energy. The second-harmonic radiation from a Nd^{3+}: YAG laser (λ_{pump} = 532 nm, E_{pump} = 15 mJ, PRF = 25 Hz) was used for excitation. The 25 mm-long active rod absorbed 98% of the pumping energy. As can be seen from Fig. 3a, the total lasing efficiency is as high as 55%, while the differential efficiency (the lasing-to-pump energy increase ratio) is 65%. This experiment suggests that a quantum laser efficiency of about 1 is feasible. Thus, in well-engineered Ti^{3+}:Al_2O_3 lasers the conversation efficiency is limited only by Stokes losses, $\eta_{st} = h\nu_{las}/h\nu_{pump}$. This experiment also confirms the fact that no observable absorption from the excited levels occurs in Ti^{3+}: Al_2O_3 and that nonradiative relaxation is unimportant under pulsed pumping conditions which are the two most critical processes limiting laser performance. The reduced effect of the latter mechanism is also confirmed by the temperature dependence of the laser pulse energy and the average output power of Ti^{3+}: Al_2O_3 lasers (see Fig. 3b). It follows from Fig. 3b that for an excitation pulse duration of 10 ns the output energy of a Ti^{3+}: Al_2O_3 laser decreases only when the active rod is heated to > 240°C, and even for a pumping pulse duration of 400 ns the limiting temperature is 180°C (Ref. 28), which is one more important advantage of Ti^{3+}: Al_2O_3 lasers. Such a wide temperature range over which the output laser energy remains constant is of great practical importance and gives this kind of laser a distinct advantage over a number of lasers based on chromium-doped crystals and, especially , those based on crystals doped with V^{2+}, Ni^2, or Co^{2+} which are capable of operating only at cryogenic temperatures.

Ti^{3+}: Al_2O_3 lasers are attractive light sources for lidars on account of their capability of delivering fairly high single-pulse energies. Experiments on lasing in Ti^{3+}: Al_2O_3 crystals pumped by second-harmonic radiation from a neodymium-glass laser have shown that the pulse energy is limited only by the output energy of the pumping source, which was, for example, 0.6 J at a pump pulse energy of E_{pump} = 2 J (Ref. 30). Comparable output energies have been obtained with dye-laser pumping (2 J at E_{pump} = 10 J) (Ref. 31). The specific stored energy of the active medium can be as high as 5 to 10 J/cm^3 at a dopant concentration of 0.1% by weight. Work is under way now to develop a Ti^{3+}: Al_2O_3 laser system with an output energy ≥ 15 J. Thus the energy potential of Ti^{3+}: Al_2O_3 lasers can meet the requirements of radiation sources for atmospheric sensing. An unfavorable aspect of these lasers, however, is the necessity of using high-energy neodymium lasers for pumping.

The fourth specific feature of Ti^{3+}: Al_2O_3 lasers is their power characteristics. The latter, as well as the energy parameters, are determined by the energy potential of the pumping source. Already in early investigations[13,24] an average output power of 1.2 W (PRF = 40 Hz, pulse energy 30 mJ) was obtained for pumping by the second harmonic of the Cr^{3+}, Nd^{3+}: GSGG lasers. Comparable average powers were obtained with pumping by a neodymium-glass laser (P_{las} = 1.3 W at E_{las} = 0.65 J, PRF = 2 Hz) and by a quasi-continuous Nd^{3+}: YAG laser.[28] For pumping by a copper-vapor laser, an average laser power of 2.6 W was obtained.[33]

We will present the scheme and the characteristics of one of the Ti^{3+}: Al_2O_3 lasers which we built that had coherent pumping and operated in the quasi-continuous regime (Fig. 4). The pumping of this laser was performed with a commercially available Nd^{3+}: YAG laser (LTI-701) with an intracavity

frequency doubler. A 6 mm-diameter and 6 mm-long Ti^{3+}: Al_2O_3 laser rod is mounted on a thermal contact of indium inside an aluminium heat sink R with radiating area 200 cm^2 and is placed at the caustic of the intracavity telescope consisting of lenses L_1 and L_2. The diameter of the active zone in the crystal was 80 μm. The pumping radiation is injected into the cavity through a spectrum divider and a dichroic mirror and is focused on the crystal with the lens L_1 (F = 65 mm). The tuning is performed using a diffraction grating (1200 grooves/mm) whose spectral selectivity is improved through the use of a prism telescope. Such a configuration provided an output power of 760 mW at the maximum of the gain band at 4 W average pump power. The tuning range obtained for a 30 μm linewidth of the laser emission was 670 to 960 nm. The output beam divergence was 0.3 mrad.

The above energy and power parameters are characteristic of single-crystal lasers and can be increased dramatically by using a more sophisticated arrangement such as those used in multistage laser systems. Let us consider the feasibility of controlling the spectral characteristics of the Ti^{3+}: Al_2O_3 lasers and, first of all, the conditions necessary for generating a narrow line in a given spectral region. As mentioned above, the broad luminescence band is fairly homogeneously broadened, and therefore highly efficient release of stored energy is possible in any spectral interval within the gain band. Note that the techniques developed for mode selection in dye and color-centered lasers[34] are also applicable to the Ti^{3+}: Al_2O_3 laser.

As an example, let us consider the spectra characteristics of a quasi-continuous Ti^{3+}: Al_2O_3 laser. The experiments cited employed the resonator geometry shown in Fig. 4a.

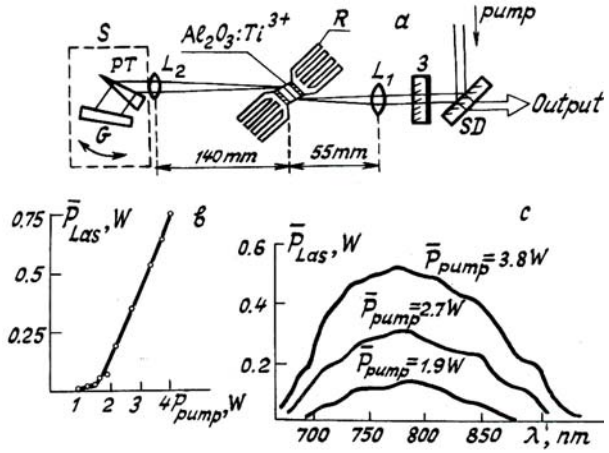

FIG. 4. Block diagram of the laser (a); average output power as a function of the average pumping power (b); tuning curves for the Ti^{3+}:Al_2O_3 laser at different energies of pumping in the quasi-cont inuous regime (c).

The selection unit (dashed contour) was modified for different experiments and the versions used are shown in Fig. 5a.

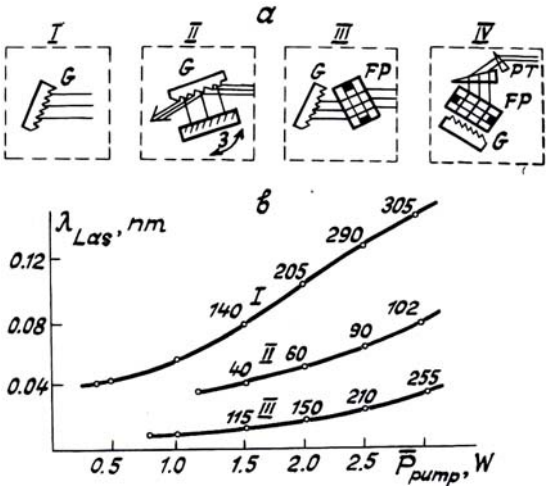

FIG. 5. Types of spectral selector used (a); dependence of the spectral width of the output emission on the pumping power for different types of selectors (b). The numbers alongside the experimental points show the output power in mW.

The laser emission spectrum width is plotted in Fig. 5b as a function of the average pumping power obtained using different selectors. It can be seen from this figure that even the use of only one diffraction grating in the auto-collimating scheme (selector type I) allows one to narrow the emission linewidth, on the average, down to 100 pm and provides lasing efficiency in excess of 10%. As noted above, the use of a single-element prism telescope with a diffraction grating narrows the laser linewidth down to 30 μm. Approximately the same results are obtained with a grazing-incidence grating and mirror combination (selector type II). However, the energy characteristics in this scheme are found to be decreased by a factor of 3. The use of a grating and etalon combination (selector type III) leads to a further reduction of the linewidth by nearly tenfold, decreasing the output energy by 20 to 30%. It is especially effective to use the combination of grating, etalon, and two-element prism telescope (selector type IV). In this case the laser linewidth is as narrow as 1 to 3 pm with a lasing efficiency of a few percent. When an additional etalon with a 22-mm spacing is used in the type-IV selector, lasing occurs on a single longitudinal mode with a bandwidth of about 0.3 pm.

Fast tuning of the Ti^{3+}: Al_2O_3 wavelength can be effected by means of opto-acoustic devices capable of controlling the lasing spectrum.[35–36] But there arises a problem with the use of opto-acoustic deflectors since they introduce great losses into the cavity. Nevertheless, the fairly large gains which are attainable in titanium-sapphire crystals make it advantageous to use deflectors for mode selection.

Thus, Ti^{3+}: Al_2O_3 lasers can emit radiation at any of the lines required for solving atmospheric sensing problems and under fast-tuning conditions.

The laser linewidth and spectral position are stabilized in the same way as in other types of lasers. In

particular, the laser line in the scheme with the type-IV selector can be stabilized to within $\Delta\lambda_{las}/2$ using a thermostatic interferometer.

The spatial characteristics of Ti^{3+}: Al_2O_3 laser radiation are determined by the cavity type used and by the excitation conditions. If the pumping laser emits only axial modes, then a nearly diffraction-limited divergence of 0.3 to 0.5 mrad (Ref. 28) can be obtained in Ti^{3+}: Al_2O_3 at a beam diameter of approximately 3 mm.

Recent findings demonstrate the feasibility of obtaining diffraction-limited beams at maximum attainable efficiency for multimode pumping as well. The spatial characteristics of the flashlamp-pumped Ti^{3+}: Al_2O_3 lasers are normally formed by the same methods as in conventional solid-state lasers. Thermal distortions are significantly lower in this case as compared, i. e., to ruby and neodymium lasers because good thermal conductivity of the host is combined here with a four-level lasing scheme, which implies the use of low pumping energy.

The polarization of Ti^{3+}: Al_2O_3 radiation is determined by the relative orientation of the crystal axis C_{3v} and the optical axis of the laser rod. The laser crystals are generally cut so that the angle between these axes lies between 60 and 90°. In this case the output radiation is completely polarized. If the optical axis of the active element is parallel to the crystal axis, the output radiation is unpolarized. The absorption conditions in Ti^{3+}: Al_2O_3 and, consequently, the excitation conditions are also dependent on the relative orientation of the polarization vector and the indicated axes. The absorption peaks when all three vectors lie in the same plane.

AMPLIFYING PROPERTIES OF Ti^{3+}: Al_2O_3 CRYSTALS

In some applications, including laser studies of the atmosphere, the use of multistage laser systems with successive amplification of the radiation is preferable since the requirements imposed in this case on the spectral, spatial, and temporal characteristics of the output radiation, in addition to high power and energy, can be better met in the master oscillator of such a laser system.

Let us consider the amplifying properties of Ti^{3+}; Al_2O_3 crystals and the feasibility of using them as a basis for high-power systems. The basic amplifier characteristics are the saturation threshold, the linear amplification factor, the loss factor, and the energy stored per unit volume of the active medium. When a continuous signal is amplified, the saturation intensity $I_s = h\nu/2\sigma\tau_{lum}$ is equal to 10^5 W/cm^2 at $\lambda = 800$ nm. For short pulses the saturation energy density $F_s = h\nu/2\sigma$ is equal to 0.7 J/cm^2. The linear amplification factor for Ti^{3+}: Al_2O_3 can be on the order of a few fractions of an inverse centimeter or a few inverse centimeters. Thus, for crystals with a dopant concentration of 0.1% by weight the linear amplification factor is about 10 cm^{-1} under conditions of complete population inversion. The nonresonant loss factor in real crystals does not exceed a few hundredths or thousandths of an inverse centimeter (Ref. 17). As already mentioned, the energy stored per cubic centimeter range from 5 to 10 J.

We have examined the amplifying properties of Ti^{3+}: Al_2O_3 under pulsed,[32] repetitively pulsed,[37] and quasi-continuous[38] pumping. Figure 6 shows some characteristics of Ti^{3+}: Al_2O_3 based amplifiers. Evidently, the amplification factor K is linearly dependent on both the input energy density (Fig. 6a) and the pumping energy density (Fig. 6b). The experimental results agree well with the calculated data and are reliably predictable, which confirms the assumption that there are no mechanisms limiting the amplification.

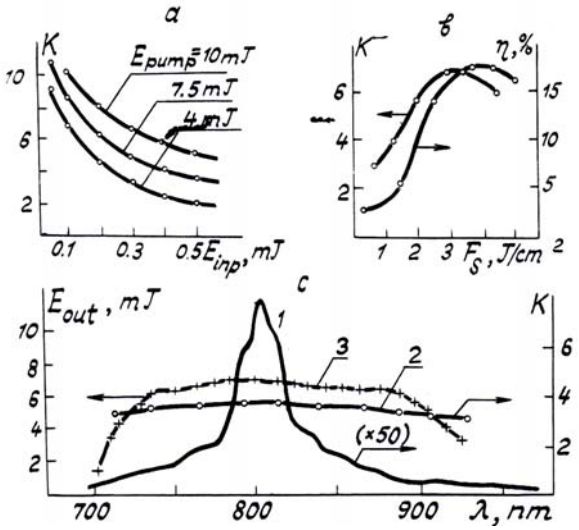

FIG. 6. Gain coefficients as functions of the input energy at different pumping energies (a); gain coefficient and efficiency as functions of the input signal energy density (b); spectral behavior of the gain coefficient for weak (1) and strong (2) signals and of the output energy of the master oscillator-amplifier of the Ti^{3+}: Al_2O_3 *system operating in the saturation mode (c).*

The spectral distribution of the amplification factor has been studied, and conditions favorable for obtaining a more uniform tuning curve have been found. Curve 1 in Fig. 6c illustrates the spectral variations of the small-signal amplification. The pulse energy at the input of the amplifier in the spectral region of interestwas constant and equal to 10^{-5} J at an energy density of $5 \cdot 10^{-2}$ J/cm^2, while the pumping energy was $1.2 \cdot 10^{-2}$ J. The spectral behavior of the linear amplification factor observed in this experiment coincides completely with the calculated behavior $K(\lambda) = \sigma(\lambda)\Delta N$. At a higher pumping energy ($3 \cdot 10^{-2}$ J) the above value of the amplification factor $K = 3 \cdot 10^3$ was achieved at the maximum of the amplifier gain band, at an input pulse energy of 10^{-6} J.

Curve 2 in Fig 6c shows the spectral dependence of the amplification factor for the case of strong

signals, $E_{input} = 10^{-3}$ J for $E_{pump} = 1.2 \cdot 10^{-2}$ J. It is noteworthy that the amplification factor is constant over the entire spectrum. This is explained by the fact that the input signal in this case is significantly higher than the saturation energy density ($F_{input} \geq 6F_s$), which provides for complete extraction of the stored energy in any portion of the spectral region. A reservation should be made at this point to the effect that the power density in the input beam at pulsewidths of 10–15 ns is close here to the laser damage threshold. For pulsewidths $\tau_{pulse} \geq 100$ ns this danger is much pulse less and such a laser regime becomes feasible. Curve 3 in Fig. 6c depicts the spectral dependence of the output energy of the master oscillator-amplifier system in the case when the master oscillator has the usual tuning characteristic (Fig. 10a) and the energy at the input to the amplifier varies from $1.5 \cdot 10^{-3}$ J at the center of the tuning curve to $3 \cdot 10^{-4}$ J at the ends of the spectral region. The total pumping energy in the master oscillator-amplifier system is 30 mJ. This spectral behavior is important from the practical point of view because it demonstrates the possibility of constructing a tunable source with a Π-shaped tuning curve.

The above spectral variations of the $Ti^{3+;}$ Al_2O_3 amplifying properties were obtained for the input signal with $\Delta\lambda = 0.5$ μm. Recent experiments on signal amplification with $\Delta\lambda = 1$–3 μm as well as on single-frequency (one longitudinal mode) operation with $\Delta\lambda \approx 0.3$ μm have shown that the principal relationships are also valid in these case.

We have succeeded in amplifying a broadband signal from the Ti^{3+}:Al_2O_3 master oscillator with a nonselective resonator ($\Delta\lambda = 75$ nm). This laser regime is characterized by certain transformations of the spectral contour (narrowing) and pulse shape.

As far as the energy characteristics of the Ti^{3+}: Al_2O_3 amplifiers are concerned, we point out that they are also determined by the performance of the pumping source and can be relatively easily scaled, thus enabling one to develop laser systems with output pulse energies of a few joules or a few tens of joules as shown in the previous section of this paper. The stored energy efficiency of the amplifier can reach 30–40% in or near the saturation regime. Since the major part of the energy is used to pump the amplifier, this implies a high total efficiency of the system.

Discussing possible ways of constructing high-power, high-efficiency Ti^{3+}: Al_2O_3 lasers, let us consider laser systems with injection of radiation. A Ti^{3+}: Al_2O_3 laser working in this regime was first demonstrated by Brockman et al. (Ref. 39). The slave laser in this case was actually a multipass amplifier providing more efficient use of the stored energy at a much lower input (injected) signal than those required for the operation of the amplifier in the saturation regime. As a result, it becomes possible to construct simple and efficient high-power systems.

We carried out a many-sided investigation of the injection regime in Ti^{3+}: Al_2O_3 lasers and now present some of the results. It should be noted at the very outset that the above regime in Ti^{3+}: Al_2O_3 lasers is fairly efficient, because of the long duration of the linear stage in the development of the laser emission. This makes it possible to realize efficient control of the laser emission spectrum in a high-power Ti^{3+}: Al_2O_3 laser with a weakly selective cavity in the spectral region 715 to 900 nm. The injector and the slave laser were pumped by the same source, which wascharacterized by the following parameters: $\lambda_{pump} = 532$ nm, $E_{pump} = 50$ mJ, $f = 50$ Hz, and $\tau \leq 15$ ns. The pumping radiation was split into two beams in the ratio 1:9. The beam with single pulse energy of about 5 mJ excited the injecting laser while the major portion of the energy (about 45 mJ) was directed into the slave laser via a controlled delay line. The mode structure of the two lasers was matched by means of an intracavity telescope. The coupling coefficient for the laser cavities was about 5.5%. In the absence of radiation the slave laser itself emitted radiation within a band 8–10 nm in width tunable over the 715 to 900 nm spectral region. Upon switching on the injection laser in the regime of optimal temporal matching of the pump pulses of both lasers, we observed full transfer of the output radiation energy of the slave laser into a line 1 to 3 pm wide whose spectral position followed that of the injection-laser radiation. The output energy from the slave laser varied only slightly over the operating spectral range and was equal to 10–13 mJ. The energy of the injected radiation required for complete control of the slave laser spectrum varied from 8 to 110 μJ over the spectral region under our experimental conditions.

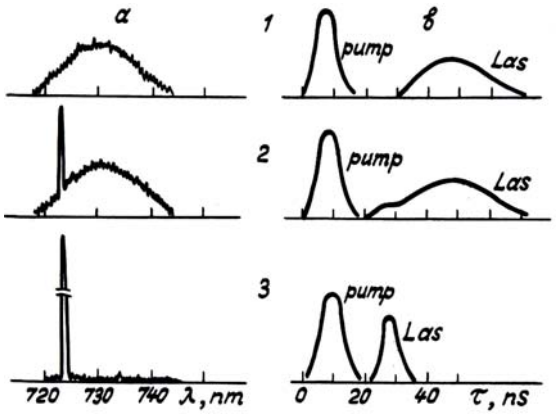

FIG. 7. Spectral (a) and kinetic (b) characteristics of the slave Ti^{3+}: Al_2O_3 oscillator: with no injected signal (curves 1); at $E_{inj} = 12$ μJ (curves 2), and at $E_{inj} = 110$ μJ (curves 3).

Figure 7 shows the evolution of the spectral and temporal characteristics of the slave laser emitting in the wavelength region of one of the analytical bands of water vapor as a function of the level of the Injected signal. In the absence of the injected signal the duration of the slave laser pulse is about 50 ns, the pulse being delayed by 70 to 80 ns with respect to the pumping pulse. The delay is related to the time it takes

to form laser radiation from the spontaneous noise. The spectral width of the laser emission band is about 8 μm When the injection laser is switched on, its effect on the slave laser spectrum and kinetics is observed already at an energy of the Injected radiation of about 25 μJ. At energies of the injected radiation ≥ 0.1 mJ the energy of the slave laser is completely transferred to the narrow line. The lasing buildup time is significantly reduced because the lasing process develops on the basis an injected signal with high spectral brightness. The simplicity and efficiency inherent in injection-locked Ti^{3+}: Al_2O_3 lasers allows us to recommend them for the construction of high-power laser systems emitting narrow-band radiation.

The above data indicate the feasibility of creating laser sources with high efficiency, high output energy, and average power adequate for the solution of practical problems which arise in laser sensing of the atmosphere. The possibility of obtaining a Π-shaped tuning curve over a broad spectral range should be particularly emphasized because it is not characteristic of known tunable sources of coherent radiation. Concluding the discussion of the amplifying properties of Ti^{3+}: Al_2O_3 crystals, we should also mention the possibility of obtaining ultrashort high-energy pulses with this type of laser. The extremely large spectral width of the gain band and the optimal saturation parameters (see above) give good reason to expect efficient femtosecond pulse amplifiers with an output energy of up to several joules.

MODES OF Ti^{3+}: Al_2O_3 LASER OPERATION

The capability of operating in different regimes is one of the most important of laser characteristics, and determines their range of application. It follows from the foregoing discussion that Ti^{3+}: Al_2O_3 lasers can lase efficiently in pulsed, repetitively-pulsed, and quasi-continuous modes. In addition, let us consider the available data on continuous and mode-locked regimes. Some of these results are presented in Refs. 28, 40, and 41. Continuous oscillation is excited either by an argon laser (we use here the two most intense lines at $\lambda_1 = 488$ and $\lambda_2 = 514$ nm) or by the second harmonic of a Nd^{3+}: YAG laser. The cw Ti^{3+}: Al_2O_3 lasers are notable for their simple design in which a three-mirror cavity similar to dye-laser cavities is commonly used or the cavity configuration shown in Fig. 4a in which the grating is replaced by a mirror and a Lyot filter is used as the selector because of its lower losses. The lasers emit at room temperatures, the threshold absorbed power being 800 mW (Ref. 28), 1300 mW (Ref. 42), and even 100 mW (Ref. 43). The output power that has been obtained so far is 1.6 W at a differential efficiency of 19% (Ref. 42). As expected, the laser efficiency and energy characteristics of the Ti^{3+}: Al_2O_3 laser in the cw mode depend, in the first place, on the quality of the crystal. Our experience with this kind of laser shows that a guiding criterion for using these crystals in cw lasers is the ratio of the peak absorption coefficient at 480 nm to the total losses (absorption + scattering) in the lasing spectral range. This ratio must be $\geq 10^2$.

Mode-locking in the Ti^{3+}: Al_2O_3 laser was first observed by Altshuler et al.[41] The early experiments using synchronous pumping yielded pulse durations 10 to 15 ps at a conversion efficiency of up to 10%. Mode-locking was produced in a weakly selective cavity with passive Q switches of dye solutions. The pulse durations of the obtained pulse trains were ≤ 25 ps. At present we have realized the regime of active mode locking using an acousto-optic modulator inside the cavity of a Ti^{3+}: Al_2O_3 laser with quasi-continuous pumping. Stable pulse trains with spikes shorter than 100 ps in width were produced in the 670 to 960 pm spectral range at a conversion efficiency of up to 30%. The mode-locked operation of the Ti^{3+}: Al_2O_3 lasers has a number of specific features which have been examined in the relevant papers. Summarizing the discussion of coherently excited Ti^{3+}: Al_2O_3 laser characteristics, Table II below lists the parameters of the currently available sapphire lasers. Naturally, the tabulated data represent advances at an intermediate stage of development.

Finally, mention should be made of a positive feature inherent in coherently pumped Ti^{3+}: Al_2O_3 lasers that of the long lifetime of the active rods. A detailed investigation of this characteristic has not been made yet, since it is determined to a considerable extent by the crystal growth technology. However, lower limits for crystals grown by a modified Kyropulos method developed by V.N. Matrosov can be given. The operating lifetime for active crystals in repetitively pulsed lasers is found to be $\geq 10^8$ pulses at an excitation power density of 30–80 MW/cm^2 while in quasi-cw lasers it is $\geq 10^{11}$ pulses (f = 25 kHz), which dramatically exceeds the lifetime of the neodymium lasers used to pump them.

Flashlamp excitation in Ti^{3+}:Al_2O_3 lasers has not been in wide use so far. This is because the Ti^{3+}: Al_2O_3 lasers are inferior to coherently excited lasers in a number of critical respects. The problems with flashlamp pumping result from the short lifetime of the upper laser level (3.7 μs). This implies the use of microsecond pumping pulses and, consequently, very severe flashlamp operating conditions, significantly reducing the flashlamp lifetime. In the microsecond operation the major portion of the pulsed emission is in the UV region and cannot be used for direct excitation of the Ti^{3+} ions in Ti^{3+}: Al_2O_3. Therefore, the very first experiments on flashlamp excitation of the Ti^{3+}: Al_2O_3 lasers[12,44–46] made use of luminophors based on dye solutions. The best results obtained so far with flashlamp excitation have been those reported by Lacovera and Esterowitz[46] who employed Coumarine 102. Their laser produced 2.5 W mean output power (125 mJ, 20 Hz), 12 J threshold energy, and a laser efficiency of up to 0.5% over the tuning range of 710 to 912 nm. The operating lifetime of the home-made flashlamps which were used was as long as $2.5 \cdot 10^5$ shots. Despite these encouraging characteristics, the laser can hardly be recommended for practical applications. Its weak point is the dye luminophor, which has a finite lifetime and requires a

dye flow circulation. For these reasons this kind of design fails to demonstrate all the advantages of the Ti^{3+}: Al_2O_3 laser associated with the optical and physical characteristics of the active medium.

TABLE II.

Lasing characteristics of the Ti^{3+}: Al_2O_3 crystal under conditions of coherent pumping.

Regime and form of pumping	efficiency tot/dif	λ_{las}, nm	E_a, J	E_{thr}, J	τ_p, s	f_p, Hz	P_{las}, Vt
Pulsed (YAG:Nd^{3+}), λ_p=532 nm	48/68	670-960	$3\cdot10^{-2}$	$0.5\cdot10^{-3}$	$(4-10)\cdot10^{-9}$	40	1.2
Pulsed (glass:Nd^{3+}), λ_p=532 nm	35/50	690-910	0.65	0.3	$(2-500)\cdot10^{-10}$	2	1.3
Quasi-continuous (YAG:Nd^{3+}), λ_p=532 nm	45/70	670-980	$0.5\cdot10^{-4}$	$0.3\cdot10^{-6}$	$(1-10)\cdot10^{-9}$	$(8-25)\cdot10^3$	0.76
Continuous (Ar-laser), λ_p=488+514 nm	7/20	680-980	—	0.8 W	—	—	0.13
Quasi-continuous, λ_p=510+578 nm	35/50	680-960	$4.5\cdot10^{-4}$	$0.5\cdot10^{-3}$	$(5-20)\cdot10^{-9}$	$5.5\cdot10^3$	2.6
Mode-locked regime (locked pumping), λ_p=532 nm	15/13	700-900	$1.5\cdot10^{-3}$	$2\cdot10^{-3}$	10^{-11}	10	$15\cdot10^{-3}$
The same (active mode-locking), λ_p=532 nm	30/45	680-960	$3\cdot10^{-5}$	10^{-5}	10^{-10}	$2.5\cdot10^4$	0.24

We have studied the feasibility of obtaining laser action from Ti^{3+}: Al_2O_3 under conditions of flashlamp excitation, using solid-state luminophors. The latter were produced from glasses doped with univalent copper and cerium, similar to those investigated by Kruglik et al. (Refs. 47 and 48) but having a higher resistance to UV radiation. The experiments used a cylindrical illuminator made of a quartz tube with an external aluminum coating. Mounted between the flashlamp and the active element was either a glass filter rejecting radiation with wavelengths shorter than 400 nm or a 2 mm-thick luminophor. The quantum efficiency of the luminophor was 85%. A 4.5 mm-diameter, 50 mm-long active element with a dopant concentration of 0.15% by weight was placed within a 50 cm-long cavity with mirror reflectivities of R_1 = 99.9% and R_2 = 85%. The pumping pulse duration (*FWHM*) was 15 μs.

The spectral characteristics of the luminophor and its effect on the laser threshold and output energy are illustrated in Fig. 8. The lasing threshold in the case of the cutoff light filter was 37 J. When the filter was replaced with the luminophor, the threshold decreased to 10 J while the differential laser efficiency increased by a factor of 4–6, which is indicative of the high efficiency of the luminophor used. The above preliminary results give an idea of possible ways to improve flashlamp-pumped Ti^{3+}: Al_2O_3 lasers.

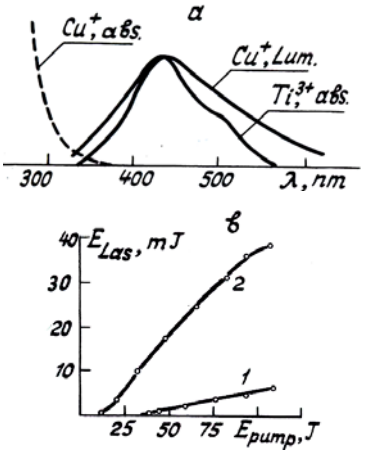

FIG. 8. Spectral characteristics of glass activated with Cu^+ ions compared with the absorption spectrum of the Ti^{3+}: Al_2O_3 crystal (a); output energy of a flashlamp pumped Ti^{3+}: Al_2O_3 laser as function of pumping energy without luminophor (1) and with it (2) (b).

Nontraditional methods of excitation. By these methods we understand the excitation by electron beams and solar radiation.

Electron beams interacting with a solid body produce electron-hole pairs. This process consumes the major part of the electrons' energy, which is normally a few hundred keV. The process of electron-hole recombination results in the excitation of the activating ions. Therefore the electron beams can be used to excite lasing in activated crystals. Experiments on excitation of laser emission in activated crystals by electron beams were carried out, for example, in Refs. 49–51, but no practical results were obtained because of either limited radiative strength of the crystals (Nd: $^{3+}Y_3Al_5O_{12}$) or the necessity of providing a high density of the excited states (Cr^{3+}: Al_2O_3 with a three-level lasing scheme).

In contrast to those media, the Ti^{3+}: Al_2O_3 crystal has an advantageous combination of high radiative strength and a 4-level lasing scheme, which has a low lasing threshold. We have carried out experiments on obtaining laser emission in Ti^{3+}: Al_2O_3 crystal pumped by electron beams, and present here some preliminary results. We were assisted in this experimental study by M.V. Belokon'.

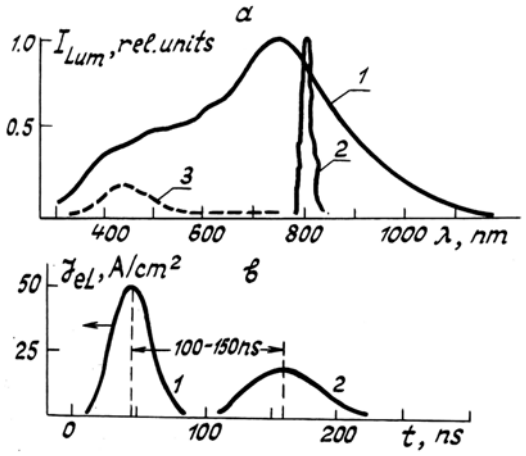

FIG. 9. The spectra of luminescence (1), lasing (2), and induced absorption (3) of a $Ti^{3+}Al_2O_3$ *crystal with electron beam excitation (a); the current pulse of the pumping electron beam (curve 1) and the* $Ti^{3+}Al_2O_3$ *laser pulse (curve 2) (b).*

The parameters of the electron beams which we used are as follows. The energy of the electrons in the beam was E_e = 200 keV, pulse duration τ_p = 50 ns, and current density J = 50 A/cm²p, and the repetition rate was f = 5 Hz. An intense luminescence was observed in a $Ti^{3+}Al_2O_3$ crystal irradiated by electron beams with the above-mentioned parameters, whose spectrum is presented in Fig. 9a. In the laser-emission experiments we used the transverse pumping arrangement. The thickness of the excited layer in the crystal was about 250 μm. The ends of a 25 mm-long $Ti^{3+}Al_2O_3$ crystal were coated with mirror layers whose reflectivity was 96%. Laser emission escaped from the cavity symmetrically through both ends of the crystal. Figure 9 presents the spectrum of the laser emission and its kinetic characteristics. The parameters of the laser radiation were practically the same after 10^5 shots, which clearly demonstrates the high radiative strength of the crystal. After multiple irradiation of the crystal by electron beams with a total exposure of 10^{17} electrons/cm² there appeared a weak absorption band at λ = 470 nm, which however did not produce any, effect on the lasing properties of the crystal. Theoretical estimations and the experimental results obtained allow us to hope that an efficiency of conversion of the energy stored in the electron beam into the laser radiation of up to 10–12% could be reached. Taking into account the simplicity of electron guns with the above-mentioned parameters, this way of creating reliable lasers working in a wide spectral range seems to be very promising.

The use of solar radiation for pumping $Ti^{3+}Al_2O_3$ lasers is of special interest. This is a result of the almost perfect matching between the solar spectrum and the absorption spectrum of the $Ti^{3+}Al_2O_3$ crystal (see Fig. 2 in Ref. 3). The maximum of the solar spectrum is near λ_{max} = 470 nm, while the maximum of the $Ti^{3+}Al_2O_3$ absorption spectrum is at 490 nm. At the same time, the wide absorption band of the $Ti^{3+}Al_2O_3$ crystal overlaps almost the entire visible range, thus providing for very efficient use of solar radiation for pumping. The spectral range between 400 and 615 nm contains about 35% of the radiant energy contained in the solar spectrum and can be effectively used for the direct excitation of the Ti^{3+} ions in the Al_2O_3 crystal matrix. In addition, the use of a luminophor of a copper-activated glass (see above) can provide a conversion (with a conversion efficiency greater than 85%) of the solar spectrum below 400 nm into radiation with wavelengths between 400 and 600 nm, which is well absorbed by $Ti^{3+}Al_2O_3$ crystal. Thus about 20% of the solar radiation energy contained in the spectral range below 400 nm can also be used for pumping. That means that about 55% of the solar radiation energy can be efficiently used for exciting the Ti^{3+} ions in the $Ti^{3+}Al_2O_3$ crystal. There are no known laser media with the exception of Ti^{3+}: Al_2O_3 which have such an attractive feature. A technique applicable for calculating the basic parameters of solar-pumped solid-state lasers can be found, for example, in Refs. 52 and 53. According to this technique, the degree of concentration of solar radiant energy ξ, required to produce lasing in solid-state lasers is determined from the threshold condition for lasing as follows:

$$\alpha_g = N\sigma_{14}(I_s\eta_{sp}\xi/\bar{h}\nu_s A_{32})(1-\xi_{thr})\sigma_{32} > \alpha_{loss} \qquad (2)$$

where α_g is the gain coefficient of the active medium; N is the number density of the active particles; σ_{14} and σ_{32} are the cross/section of the absorption on the transition 1→4 and amplification on the transition 3→2, respectively; I_s is the solar constant, which is equal to the power density of the solar radiation at the Earth's surface ($I_s \approx 0.1$ W/cm²); η_{sp} is the fraction of the solar spectrum absorbed by the activating

particles in the transition 1→4; $\bar{\nu}_s$ is the mean frequency of the solar radiation absorbed by the medium; A_{32} is the rate of decay of the upper lasing level; α_{loss} is the total energy losses at the lasing frequency;

$$\xi_{thr}^{r} = \frac{g_3 h\bar{\nu}_s A_{32} \exp(-\Delta F_{21}/kT)}{g_2 \sigma_{14} I_s \eta_{sp}}, \quad (3)$$

where ξ_{thr}^{r} is the threshold degree of concentration of solar radiation required to obtain population inversion in the lasing transition 3→2; g_2 and g_3 are the degeneracies of the corresponding energy levels; and ΔE_{21} is the energy gap between the ground level and the lower lasing levels. The right part of Inequality (2) stands for losses which, for simplicity, are considered to be due to diffraction $\alpha_{dir} \approx \lambda_{32}/l^2$, (where λ_{32} is the wavelength of the laser emission, l is the transverse diameter of the active medium) and scattering and inactive absorption α_{in}.

Let us estimate ξ_{thr}^{r} for the $Ti^{3+}Al_2O_3$ crystal. The parameters necessary to make this estimate are $\alpha_{in} = 3 \cdot 10^{-3}$ cm^{-1}; $\lambda_{32} = 0.8$ μm; $\bar{\nu}_{32} = 0.8$ μm; $\bar{\nu}_s = 6 \cdot 10^{14}$ Hz; $\eta_{sp} = 0.55$; $\sigma_{14} = 8 \cdot 10^{-20}$ cm^2; $\sigma_{32} = 35 \cdot 10^{-19}$ cm^2; $A_{32} = 27 \cdot 10^{-5}$ s; $g_2 = 3$; $g_1 = 1$; $\Delta E_{21} = 4230$; 2000 cm^{-1} (see Fig. 1a). At $\Delta E_2 = 2000$ cm^{-1} and under the condition that all the pumping energy is absorbed ($N\sigma_{14}l \geq 1$) we obtain $\xi_{thr}^{r} \geq 6 \cdot 10^3$ if the concentration of Ti^{3+} ions is $\sim 10^{20}$ cm^{-3} (or 0.3% by weight) and the cross-sectional diameter of the crystal is 2–3 mm. Such a concentration of solar energy is, in principle, possible, though it is too difficult technically to achieve it. Nevertheless, even the technology of crystal growth available now (Ti^{3+}: Al_2O_3 crystals with $\alpha_{in} = 3 \cdot 10^{-3}$ cm^{-1}) makes it possible to consider the creation of a solar-pumped Ti^{3+}: Al_2O_3 laser to be a realistic task. The situation changes for the better if one uses waveguide lasers of Ti^{3+}: Al_2O_3 crystals which have lower inactive and diffraction losses and takes into account the possibility of using the laser scheme with $\Delta E_{21} = 4230$ cm^{-1}. In this case the value ξ_{thr}^{r} can be reduced to 10^2 and lower, which enables one to obtain this degree of concentration of solar radiation energy using a parabolic-cylindrical concentrator. This, in turn, should make it possible to use active elements several meters long, and thus to realize not only low-threshold but also high-power Ti^{3+}: Al_2O_3 lasers with solar pumping.

Let us estimate the limiting value of the efficiency of a solar-pumped Ti^{3+}: Al_2O_3 laser:

$$\eta = \eta_{sp} \cdot \eta_q \cdot \eta_{lum},$$

where $\eta_{sp} = 0.55$; $\eta_q = \nu_{las}/\bar{\nu}_s = 0.62$; η_{lum} is the quantum yield of luminescence and is equal to 0.8. Thus we obtain $\eta = 30\%$. The specific mean power of the solar-pumped Ti^{3+}: Al_2O_3 laser (i.e., the output power of the laser per unit area of the solar radiation concentrator) then is

$$\bar{P}_{spec} = I_s \eta = 300 \text{ W/m}^2.$$

Under extraterrestrial conditions this power can be increased up to 450 W/m^2. So it is possible to conclude that the solar-pumped Ti^{3+}: Al_2O_3 laser is superior to other solar-pumped lasers by its limiting efficiency and power output per unit area of the solar energy concentrator.

Bearing in mind that the solar-pumped $Ti^{3+}Al_2O_3$ laser itself can be used for pumping some other active medium (especially if one takes into account its tunability), it can become a basic element of a multifunctional laser system (technological, remote sensing), especially a spaceborne one.

THE SPECTRAL RANGE OF THE LASER EMISSION OF Ti^{3+}: Al_2O_3 AND SOME POSSIBILITIES OF EXTENDING IT

Its extremely wide luminescence band, which is homogeneously broadened and the absence of light absorption from its excited states render the $Ti^{3+}Al_2O_3$ crystal a suitable basis for creating a tunable laser with a tuning range much wider than those of presently known lasers. At present there already exist Ti^{3+}: Al_2O_3 lasers capable of operating in all practically useful regimes and with tuning ranges from 670 to 980 nm (see Table II). A tuning curve which we have obtained using a pulsed-periodic laser Is shown in Fig. 10a. It should be noted that tuning curves can strongly differ from one another depending on cavity selectivity and the dynamics of excitation. Thus, for pumping by continuous radiation or by microsecond pulses the long-wavelength wing of the curve is, as a rule, better developed. Also, the opto-physical properties inherent in the active medium affect the shape of the tuning curve. The strongest effect on the tuning curve comes from resonance spatial structures, which can appear in the crystal during the growth process. [13,22,54] Without a question, uncontrolled impurities in the active medium can also influence the shape of the tuning curve. It is interesting to note that in this case the Ti^{3+}: Al_2O_3 laser works as an intracavity laser spectrometer. The latter circumstance forces us to analyze the conditions of Ti^{3+}: Al_2O_3 crystal growth with especial care.

As was mentioned above, we have obtained in our experiments amplification of light at $\lambda = 1.06$ and 1.15 μm quite sufficient to produce lasing. The results of experiments on the tuning of the radiation of a Ti^{3+}: Al_2O_3 laser within the range from 0.60 to 1.024 μm can also be found in Ref. 43.

In our opinion, the tuning range from 0.64 to 1.35 μm is feasible in Ti^{3+}: Al_2O_3 lasers. In this case the tuning range is a little bit wider than an octave, which suggests the unique possibility of using nonlinear crystals to widen the tuning range of the laser. Thus, frequency doubling with nonlinear crystals provides a tuning range from 320 to 675 nm whose long-wavelength wing overlaps with the short-wavelength wing of the primary tuning range. One nonlinear crystal suitable for doubling the frequency of

Ti^{3+}: Al_2O_3 radiation over its entire tuning range is $LiIO_3$ (synchronism *oo-e*). Experiments[13,28,24,25,26] on frequency doubling of Ti^{3+}: Al_2O_3 radiation with a $LiIO_3$ crystal have demonstrated a conversion efficiency up to 22%.

On the other hand the fact that Ti^{3+}: Al_2O_3 radiation is tunable over an octave makes it possible to obtain tunable radiation in the long-wavelength range starting from 1300 nm by generating radiation at difference frequencies $\nu_d = \nu_s - \nu_l$, where ν_s and ν_l are frequencies lying in the short- and long-wavelength portions of the Ti^{3+}: Al_2O_3 laser tuning range. In this process the long-wavelength boundary of the converted radiation is determined by the transmission range of the nonlinear crystal and can reach 15 to 20 μm. For example, the use of a $LiIO_3$ crystal can provide a tuning range from 1.3 to 5.5 μm. When performing such kinds of frequency conversion, one should keep in mind some peculiarities of the temporal characteristics of Ti^{3+}: Al_2O_3 laser radiation. As has already been pointed out in Refs. 25 and 28, the output pulse of a Ti^{3+}: Al_2O_3 laser is delayed with respect to the single pumping pulse by tens of nanoseconds. For quasistationary pumping the delay can increase up to hundreds of nanoseconds or more. In addition, one should take into account the fact that the pulse duration varies over the tuning spectrum by several fold.[28] This creates certain difficulties in the temporal matching of pulses at different wavelengths, which is required for good conversion efficiency. Obviously this difficulty is most severe in the case in which radiation is produced at the sum and difference frequencies (additive conversion) since in this case one must use radiation pulses from different sources, which can have different temporal characteristics as, for example, in the case with the tunable radiation of the Ti^{3+}: Al_2O_3 laser and the radiation of the pumping laser. It is precisely for this reason that the techniques suggested in Ref. 55 for widening the tuning range of the Ti^{3+}: Al_2O_3 laser by summation or subtraction of its frequency with the frequency of Nd^{3+}: YAG radiation (including its second harmonics) are not very effective.

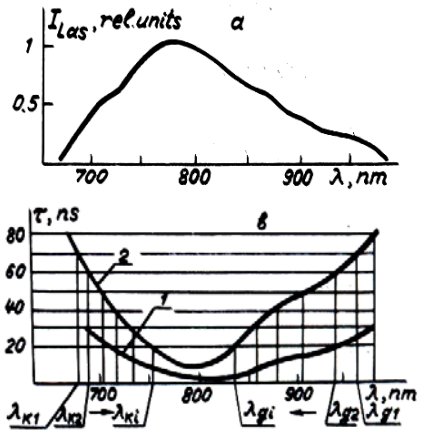

FIG. 10. Spectral behavior of the output energy of a pulsed-periodic Ti^{3+}: Al_2O_3 laser pumped with the second harmonic of the Ti^{3+}: Al_2O_3 laser (a), its pulse duration (curve 1), and delay time with respect to pumping pulse (curve 2) (b).

We propose a technique for producing radiation at the difference frequency which is free of these disadvantages. The technique is based on the taking into account of the spectral regularities of the delay process as well as on making use of the capability of the Ti^{3+}: Al_2O_3 laser to operate as a polychromator.[56] For the laser whose tuning curve is given in Fig. 10a we have measured the pulse durations and delay times relative to the pumping pulse. Results of these measurements are presented in Fig. 10b. The pulse durations were measured at half-maximum while the delay time was measured between the pulse maxima. As can be seen from this figure, the spectral dependences of these characteristics are the opposite of that of the tuning curve.

The polychromator regime of the operation of the Ti^{3+}: Al_2O_3 laser provides the possibility of obtaining emission at several wavelengths simultaneously with Independent control of each of them. In our case it is sufficient to have emission at two wavelengths.

The emission of tunable radiation at a difference frequency in the range on the long-wavelength side of 1300 nm is realized as follows. Two spectral lines emitted simultaneously from the Ti^{3+}: Al_2O_3 laser are mixed and subtracted in a nonlinear crystal. The wavelengths of these two emissions are then synchronously tuned so that the shorter wavelength increases from λ_s to λ_{s1} while the longer one decreases from λ_1 to λ_{11} as shown by the arrows in Fig. 10b. The tuning is done in such a way that it ensures the equality of the pulse durations and the delay times with respect to the pumping pulse at λ_s and λ_1. Only in this case can the maximum efficiency of the conversation be achieved, owing to full matching between the time parameters of the mixed emissions. For λ_s = 650 nm and λ_1 = 1300 nm the difference wavelength will equal 1300 nm, and then as λ_s and λ_1 are tuned toward each other the difference wavelength increases. The increase in the difference wavelength is limited only by the properties of the nonlinear converter.

Thus, the use of frequency summation and subtraction of Ti^{3+}: Al_2O_3 laser radiation in nonlinear crystals can provide a highly efficient source of coherent laser radiation tunable in the range from 0.32 to 20 μm. If radiation with shorter wavelengths is needed for some applications such as, e.g., remote sensing of ozone, it is possible to convert the Ti^{3+}: Al_2O_3 laser radiation to the third harmonic, thus extending the short-wavelength boundary of the tuning range down to 220 nm. The emissions required for this from the Ti^{3+}: Al_2O_3 laser (i.e., the primary emission and its second harmonic) have almost the same characteristics, and can be realized by simple means with high efficiency.

Summing up the above discussion, we should like to emphasize that the Ti^{3+}: Al_2O_3 lasers provide a good basis for creating highly efficient sources of coherent radiation useful in measurements of atmospheric aerosol and the monitoring of gaseous components as well as in monitoring the thermodynamic parameters of the atmosphere and a number of other atmospheric parameters.

In this regard, we feel that there is sufficient basis to recommend Ti^{3+}: Al_2O_3 lasers as basic radiation sources for use in atmospheric sensing devices. Of course, many of the promising properties of the Ti^{3+}: Al_2O_3 laser have been demonstrated only under laboratory conditions, and a detailed investigation of them is yet needed, but further efforts in these directions are justified by the advantages this light source can provide in many applications.

In conclusion I should like to acknowledge Academician V.E. Zuev for fruitful discussions which stimulated this work, also I thank Professor G.S. Kruglik and my other coauthors for the contributions to this work which made it possible to present this paper. Finally, I acknowledge Professor G.B. Altshuler, who read the manuscript and made quite useful remarks.

REFERENCES

1. V.E. Zuev, *Laser Meteorologist* (Gidrometeoizdat, Leningrad, 1974).
2. *Laser Monitoring of the Atmosphere*, ed. by E.D. Hinkley [Russian translation ed. by V.E. Zuev] (Mir, Moscow, 1979).
3. R.M. Measures, *Laser Remote Sensing* (Wiley, New York, 1984).
4. I.V. Samokhvalov et al., *Laser Sensing of the Troposhere and the Underlying Surface* (Novosibirsk, Nauka, 1986).
5. *Multifunctional Lidar Systems*, ed. by Malevich (Minsk State University, Minsk, 1986).
6. A.A. Kaminskii, Phys. Stat. Sol. (a) **87**, No. 1, 11 (1985).
7. P.F. Moulton, Laser Focus **19**, No. 5, 83 (1983).
8. V.V. Osiko, Izv. Akad. Nauk SSSR, Ser. Fiz., **51**, No. 8, 1285 (1987).
9. L.G. De Shaser, Laser Focus **23**, No. 2, 54 (1987).
10. A.M. Prokhorov, Usp. Fiz. Nauk **148**, No. 1, 7 (1986).
11. P.F. Moulton, Optic News, No. 6, 9 (1982).
12. B.K.Sevast'yanov, Kh.S.Bagdasarov, E.A.Fedorov, et al., Kristallografiya **29**, No. 5, 963 (1982).
13. G.S.Kruglik, G.A.Skripko, and A.P.Shkadarevich, *Tunable Lasers in Activated Crystals*, Minsk, Preprint of VPI of Acad. Sci. BSSR (1984).
14. Kh.S.Bagdasarov, Yu.M.Krasilov, N.T.Kuznetsov, et al., Dokl. Akad. Nauk SSSR **282**, No. 4, 848 (1985).
15. P. Albers, E. Stark, and G. Huber, J. Opt. Soc. Amer. B **3**, No. 1, 134 (1986).
16. E.K. Belonogova, A.A. Kazakov, and S.V. Shavkunov, *Electronics Reviews, Part 2, Lasers and Optoelectronics* (Moscow, Central Research Inst. "Elektronika," No. 6 (1190) (1986).
17. E.K. Belonogova, Yu.Zh. Isaenko, and S.V. Shavkunov, *Electronics Reviews, Part 2, Lasers and Optoelectronics* (Moscow, Central Research Inst. "Elektronika," No. 1 (1344), 1988.
18. E.P. Nelson, J.Y. Wong, and A.L. Shawlow, Phys. Rev. **156**, No. 2, 298 (1967).
19. R.-M. Macfarlane, J.Y. Wong, and M.D. Sturge, Phys. Rev. **166**, No. 2, 250 (1968).
20. B.F. Gachter and J.A. Koningstein,J. Chem. Phys. **60**, No. 5, 2003 (1974).
21. P.F. Moulton, J. Opt. Soc. Amer. B 3, No. 1, 125 (1986).
22. G.A. Skripko and A.P. Shkadarevich, *Physics and Spectrography of Laser Crystals* (Nauka, Moscow, 1986).
23. J.C. Walling, O.G. Peterson, H.P. Jenssen, et al., IEEE J. Quant. Electron. **16**, No. 5, 1302 (1980).
24. G.S. Kruglik, G.A. Skripko, A.P. Shkadarevich, et al., Zhur. Prikl. Spektrosk. **42**, No. 1, 126 (1985).
25. G.S. Kruglik, G.A. Skripko, A.P. Shkadarevich, Kvant. Elektron. **13**, No. 5, 1207 (1986).
26. G.S. Kruglik, G.A. Skripko, A.P. Shkadarevich, Proc. Third Inti. School on Laser Applications in Atomic Molecular and Nuclear Physics, Vilnius, 1986, p. 563.
27. G.S. Kruglik, G.A. Skripko, A.P. Shkadarevich, *The 8th All-Union Symposium on Spectroscopy of Crystals Activated with Transition Metals*, Conf. Abstracts, Part 1, Sverdlovsk, 1985, p. 120.
28. G.S. Kruglik, G.A. Skripko, A.P. Shkadarevich, et al., Zhur. Prikl. Spektrosk. **45**, No. 4, 567 (1986).
29. G.S. Kruglik, G.A. Skripko, A.P. Shkadarevich, et al., *Abstracts of Reports at the 5th All-Union Conference "Lasers Optics"*, (Vavilov State Optical Institute, Leningrad, 1987).
30. G.S. Kruglik, G.A. Skripko, A.P. Shkadarevich, et al., Izv. Akad. Nauk SSSR, Ser. Fiz. **52**, No. 6, 1236 (1988).
31. *Tunable Solid-State Lasers II, Proceedings of the OSA Topical Meeting, Ripling River Resort, Zigraz, Oregon,* Springer-Verlag, Berlin, 1986, p. 387.
32. G.A.Skripko, S.G.Bartoshevich, and E.V.Gulevich, *Abstracts of Reports at the 10th All-Union Symposium on Laser and Acoustic Sensing of the Atmosphere,* Tomsk (1989).
33. S.G. Bartoshevich, V.V. Zuev, Yu.S. Mirza, et al., Kvant. Elektron. **16**, No. 2, 212 (1989).
34. S.P. Anokhov, T.Ya. Marusiĭ, and M.S. Soskin, *Tunable Lasers* (Radio i Svyaz', Moscow, 1982).
35. V.I. Kravchenko, V.M.Moskalev, S.Yu.Oboznenko, et al., Pis'ma Zh. Tekh. Fiz. **8**, No. 3, 174 (1982).
36. A.V. Shestakov, V.A. Zhitnyuk, A.V. Lukin, et al., *Abstracts of Reports at the 5th All-Union "Laser Optics" Conference*, Leningrad, 1986, p. 245.
37. G.A.Skripko, S.G.Bartoshevich, and E.V.Gulevich, Zh. Prikl. Spektrosk. **50**, No. 3, 453 (1989).
38. S.G. Bartoshevich, V.D. Burlakov, V.V. Zuev, et al., *Reports at the 10th All-Union Symposium on Laser and Acoustic Sensing of the Atmosphere,* Tomsk (1989).
39. P. Brockman, C.H. Bair, J.C. Barnes, et al., Opt. Lett. **11**, 712 (1986).
40. A.A.Afanas'ev, L.P.Zharikhina, N.V. Kondratyuk, et al., *Abstracts of Reports at the 13th International Conference on Coherent and Nonlinear Optics*, Minsk, Part IV, 1988, p. 53.
41. G.B. Altshuler, V.B. Karasev, N.V. Kondratyuk, et al., Pis'ma Zh. Tekh. Fiz. **13**, 779 (1987).

42. A. Sanchez, R.E. Fahey, A.J. Strauss, and R.L. Aggarwal, *Tunable Solid-State Lasers II* (Springer-Verlag, Berlin, 1986), p. 202.
43. P. Albers, H.P. Jenssen, G. Huber, and M. Kokta, *Tunable Solid-State Lasers II* (Springer-Verlag, Berlin, 1986), p. 208.
44. B.K. Sevost'yanov, KH.S. Bagdasarov, E.A. Fedorov, et al., Dokl. Akad. Nauk SSSR **282**, No. 6. 1357 (1985).
45. P. Lacovara, L. Esterowitz, and R. Allen, Opt. Lett. **10**, No. 6, 273 (1985).
46. P.Lacovara and L.Esterowitz, *Tunable Solid-State Lasers II*, (Springer-Verlag, Berlin, 1986), p. 240.
47. G.S. Kruglik, G.A. Skripko, A.P. Shkadarevich, et al., Opt. Spektrosk. **59**, No. 4, 727 (1985) [Opt. Spectrosc. **59**, No. 4, 439 (1985)].
48. G.S. Kruglik, G.A. Skripko, A.P. Shkadarevich, et al., Luminescence **34**, 343 (1986).
49. Yu.A. Voron'ko, E.L. Nolle, V.V. Osiko, et al., Pis'ma Zh. Tekh. Fiz. **13**, No. 3, 125 (1971).
50. M.V. Belokon', G.S. Kruglik, and G.A. Skripko, Zh. Prikl. Spektrosk. **38**, No. 5, 752 (1983).
51. *Investigation into the Lasing Properties of Condensed Media Excited by Electron Beams, Report on Contract No. GR 028330009796,* Minsk (1986).
52. A.L. Golger and I.I. Klimovskii, Kvant. Elektron. **11**, No. 2, 233 (1984).
53. V.M. Batenin, A.L. Golger, and I.I. Klimovskii, Kvant. Elektron. **8**, No. 3, 634 (1981).
54. G.S. Kruglik, G.A. Skripko, A.P. Shkadarevich, et al., *Abstracts of Reports at the 12th All-Union Conference on Coherent and Nonlinear Optics* (Izdat. MGU [Moscow State Univ. Press], Moscow, 1985).
55. D.V. Bakin, L.M. Dorozhkin, Yu.I. Krasilov, et al., Opt. Spektrosk. **64**, No. 1, 177 (1988) [Opt. Spectrosc. **64**, No. 1, 105 (1988)].
56. G.S. Kruglik, P.N. Nasarenko, N.V. Okladnikov, et al., *Reports of the 10th All-Union Symposium on Laser and Acoustic Sensing of the Atmosphere,* Tomsk (1989).